Robotics and Autonomous Systems 145 (2021) 103848

Contents lists available at ScienceDirect

Robotics and Autonomous Systems

journal homepage: www.elsevier.com/locate/robot

# A novel search and survey technique for unmanned aerial systems in detecting and estimating the area for wildfires

Mrinmoy Sarkar [a], Xuyang Yan [a], Berat A. Erol [a,b], Ioannis Raptis [a], Abdollah Homaifar [a,*]

[a] Electrical and Computer Engineering Department, North Carolina A&T State University, 1601 East Market Street, Greensboro, NC, 27401, United States of America

[b] Computer Engineering Department, Izmir Institute of Technology, Gulbahce Yerleskesi, Urla, Izmir, 35430, Turkey

ARTICLE INFO

*Article history:*
Received 21 July 2020
Received in revised form 20 May 2021
Accepted 15 July 2021
Available online 4 August 2021

*Keywords:*
UAV
Multi-agent autonomous system
AMASE
Search & survey
Collaborative operation
Robotics

ABSTRACT

In recent years Unmanned Aerial Vehicles (UAVs) have progressively been utilized for wildfire management, and are especially in prevalent in forest fire monitoring missions. To ensure the fast detection and accurate area estimation of forest fires, a two-step search and survey algorithm for multi-UAV system is proposed to address these fire scenarios. Initially, a grid-based partition method is applied to divide the area-of-interest into several search areas. Then, an archetype search pattern is used to provide timely UAV exploration within those sub-areas. Once the fire zones are detected, a novel survey strategy is employed for UAVs to discover the boundary points of the fire zones, so that the area of the fire zones can be estimated using the sampled boundary points. In addition, the effect of wind is accounted for improving fire zone boundary estimates. The proposed search-and-survey procedure is validated on multiple simulated scenarios using the U.S. Air Force's mission-realistic Aerospace Multi-Agent Simulation Environment (AMASE) software. Simulation results showcase that the proposed search pattern can effectively discover the seeded fire zones within 40 min of the mission. This is relatively faster than the other two well-known search patterns. Moreover, the proposed survey technique provides a coverage estimate with at least 85% accuracy for the area of interest within 90 min of the mission.



## 1. Introduction

Wildfires cause significant economic loss and destructive impact in the natural environment. As a result there is increasing interest in research pertaining to forest fire monitoring. The increased number of wildfires has significantly decreased the world forest footprint and harmed the ecosystem, resulting in many other natural disasters like floods, sandstorms, and landslides [1–5]. Indisputably, the catastrophic damage caused by wildfires pose a severe threat to human life and the natural environment.

With recent developments in the science of autonomy and robotics, Unmanned Aerial Vehicles (UAVs) are able to be deployed in diverse monitoring missions including fire detection, area estimation, and fire fighting [6]. Different wildfire monitoring systems based on a singleton UAV with advanced sensor technologies are proposed in [7–13] to address this technological challenge. However, the reliability of single-UAV systems are highly limited because of the unforeseen contingencies and demanding conditions that take place during wildfires. Because a single UAV takes a longer time to explore the region-of-interest, a team of UAVs with high-performance sensors are generally more preferred in performing the fire search mission collaboratively.

Recently, a team of UAVs was utilized to reduce the risks of human operators in the detection and area estimation of forest fires [1,14–19]. In [14,16] a combination of UAVs and Unmanned Ground Vehicles (UGVs) worked collaboratively to perform fire detection and firefighting tasks. Considering the power constraint of UAVs, the UGVs serve as ground stations to continuously supply the UAV units with power and coordinate the search trajectory of the UAVs. Instead of using a team of UGVs and UAVs, the systems proposed in [17] and [18] carry out the forest fire monitoring with multiple cooperative UAVs. In [17] a three-stage procedure that consists of search, confirmation, and observation is proposed. A fault-tolerant cooperative control strategy for multiple UAVs is introduced in [18] to handle potential faults of individual, or multiple UAVs, in fire detection and area estimation missions. Furthermore, a fire spread model has been introduced to generate the trajectories of UAVs to survey the boundary of

The code (and data) in this article has been certified as Reproducible by Code Ocean: (https://codeocean.com/). More information on the Reproducibility Badge Initiative is available at https://www.elsevier.com/physical-sciences-and-engineering/computer-science/journals.

* Corresponding author.
*E-mail addresses:* msarkar@aggies.ncat.edu (M. Sarkar), xyan@aggies.ncat.edu (X. Yan), beraterol@iyte.edu.tr (B.A. Erol), iraptis@ncat.edu (I. Raptis), homaifar@ncat.edu (A. Homaifar).

https://doi.org/10.1016/j.robot.2021.103848

fire zones. In [19] the authors approached the fire search problem via the Travel Salesman Problem (TSP) and utilized a Genetic Algorithm to generate an optimal search trajectory, which comes with high computational complexities.

As mentioned above, most existing studies in wildfire monitoring using unmanned systems either rely on a single UAV, or a combination of UAVs and UGVs. Although some works have been conducted on the application of multiple UAVs in forest fire monitoring, there are still several open and critical challenges:

- The time to discover a fire zone is proportional to the size of the region of interest and inversely proportional to the number of available UAVs. Hence, it takes longer operational time to discover fire zones in the large forest with limited number of UAVs.
- The elliptical/circular fire spread model widely used in literature generates a path for UAVs to survey the boundary of fire zones. However, forest fires usually have arbitrary and irregular footprints, making it difficult to obtain an accurate estimate of the fire zones.
- The irregular shapes of fire zones potentially increase the operating time of UAVs inside those fire zones during the boundary surveying procedure. This may result in the loss of UAVs with a higher probability.
- The boundaries of the fire zones are expanding and shifting with the change of wind direction. This phenomenology makes the accurate area estimation of fire zones more difficult to pinpoint.

In order to solve these challenges, we introduced a search and survey procedure for the detection and area estimation of wildfires using a team of heterogeneous UAVs. The major characteristics of the proposed search and survey technique are highlighted as follows:

- A novel search pattern is proposed to conduct the search of fire zones by dividing the area-of-interest into smaller grid cells. Compared with existing exhaustive search patterns this manages to achieve faster detection of fires zones when the number of UAVs is limited.
- A new survey strategy of UAVs is proposed here to effectively identify the boundaries of the fire zones without the oversimplified assumption that the fire zones follow some regular geometrical shapes.
- A clustering algorithm is used to combine the sampled boundary points from different UAVs to estimate the area of a fire zone.
- The effect of the wind speed and its direction are considered in capturing the movement of fire zones over time thus improving the area estimation of the fire zones.

The remainder of this paper is organized to illustrate the following: a mathematical formulation of the problem which is described in Section 2, and a literature review of several well-known search patterns for multiple UAVs highlighted in Section 3. Section 4 discusses the details of the proposed search framework and introduces an innovative survey strategy to identify the boundary of fire zones. Several simulation scenarios are described in Section 5, and the performance of the proposed method is presented in Section 6. Concluding remarks and future works are discussed in Section 7.

## 2. Problem description

In this section, the basic definitions and problem description are provided to elucidate the scope of this work.

According to the specifications in the AMASE simulation interface [20], four basic definitions about the characteristics of the benchmark UAVs are described below.

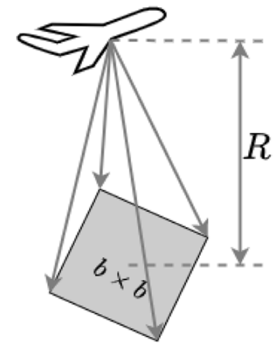


**Fig. 1.** Illustration of the fire detection sensor.

**Fire detection sensor:** A binary detection sensor is used to generate an interrupt signal when the fire appears in the field of view of the sensor. The footprint of the sensor is a square with a $b \times b$ area ($m^2$) and its range is $R$ ($m$) as shown in Fig. 1.
**Sprint UAVs:** A fixed-wing UAV with a maximum speed of $V_{sp}$ (m/s) and a fire detection sensor range of $R_{sp}$ ($m$).
**Survey UAVs:** A second type of slower, fixed-wing UAVs with a maximum speed of $V_{su}$ (m/s) and a fire detection sensor range of $R_{su}$ ($m$).
**Fire Zone:** A set of 2$D$ points (latitude and longitude) in space, consisting of the corner points of an irregular polygon.

Let $A$ be the area-of-interest in a forest. The map of $A$, referenced with respect to the Geodetic coordinate system, provides relevant terrain (altitude for a given latitude and longitude) information. The area $A$ has a set of $n$ discrete fire zones $\{fz_1, fz_2, \ldots, fz_n\}$ with respective areas $\{a_1, a_2, \ldots, a_n\}$, where $a_i \subset A$, $\forall\, i \in \{1, 2, \ldots, n\}$; $fz_i \cap fz_j = \emptyset$ for every $i, j \in \{1, 2, \ldots, n\}$ with $i \neq j$; and $\sum_{i=1}^{n} \cup a_i \subset A$. The $n$ fire zones are randomly distributed in the area-of-interest $A$ at unknown locations. It is assumed that there are $p$ *sprint* and $q$ *survey* UAVs denoted as $UAV_i$, where $i \in \{1, 2, \ldots, p+q\}$ with $p > q$, randomly placed inside the area $A$. To seek a low-cost, efficient, and fast-responsive system to perform fire search and track missions, a group of heterogeneous UAVs [21] are considered for use in the fire monitoring missions. In real-world scenarios, high-performance UAVs are expensive, and the overall operational cost will increase. Therefore, it is preferred to use a group of heterogeneous UAVs with varying capabilities to perform forest fire monitoring missions. Since the area-of-interest is large, UAVs are divided into groups, and these groups of UAVs are placed in different locations so that UAVs can perform a more effective exploration even with limited fuel and sensor capabilities. In this study, three principal problems are considered:

1. How the $p$ *sprint UAVs* and $q$ *survey UAVs* will search the area $A$ for those $n$ fire zones within the time interval of duration $T$?
2. When a fire nest is detected, how the UAVs will estimate the area of the detected fire zone areas?
3. How the $p$ *sprint UAVs* and $q$ *survey UAVs* will coordinate during the search and estimation mission?

While carrying out the search and survey missions, it is assumed that the UAVs (both types) crash to the ground if the following conditions are met:

1. Flying outside of area $A$ for a $\Delta t$ time interval.
2. Flying on top of any fire zone $fz_i$ for a $\Delta t$ time interval.
3. Flying without considering the topography of the area $A$ (e.g., flying in low altitude, colliding with mountains or trees).

## 3. Literature review

This section provides a review of several existing and well-known search patterns for fire search missions using multi-agent autonomous systems. Also, several well established survey strategies for the boundary tracking of fire zones are discussed.

### 3.1. UAV search patterns for fire detection

As one of the most popular search strategies, *Random walk* was first proposed to describe a series of random steps in the search-space [22], and has been commonly adopted for teams of UAVs to search for targets in large areas. Fig. 2(a) provides an illustration of the random search procedure with a group of UAVs. As shown in Fig. 2(a), the *Random walk* simply generates the trajectory for UAVs to move in arbitrary directions, and it does not require any prior information about the locations of targets. Because of this property, the *Random walk* is easy to implement for UAVs to search fires in an unknown area. In [23–27] a number of *Random walk*-based search approaches are developed for the search of targets with a swarm of UAVs. However, the performance of the *Random walk* becomes less desirable if targets are distributed sparsely in a large search region.

As an alternative to the random search pattern, deterministic search strategies [27,28] are studied to explore the area-of-interest by following several common search patterns [29]. In [30] the *Creeping Line*, or *Lawn Mowing*, pattern was first used for aircraft performing emergency search and rescue missions. Several recent variations of *Creeping Line* have been investigated in [31–33] for cooperative search missions using multi-agent autonomous systems. The *Creeping Line* search pattern has been widely used for coverage path planning problems; comprehensive literature for this pattern is well documented in [34]. An illustration of the *Creeping Line* search pattern is shown in Fig. 2(b). In Fig. 2(b), the search region is decomposed into a number of line segments, and the *Creeping Line* search pattern scans the whole search region by following those lines. Unlike the *Random Walk* search, the *Creeping Line* conducts an exhaustive search and, thus, it is more likely to comprehensively cover the entire search space. Clearly, the width between the consecutive scanning corridors has a direct effect on the search performance. It causes a slow exploration of the entire search area and requires more energy consumption because of its exhaustive path.

*Expanding Squares search* is another type of deterministic search patterns that is widely used in the search and rescue tasks for teams of UAVs [35]. Unlike the *Creeping Line* strategy, the entire search region is divided into a set of square layers with increasing sizes. An example of the *Expanding Squares search* for multi-UAVs system is shown in Fig. 2(c). From Fig. 2(c) multiple UAVs are assigned to follow different layers of the expanding squares simultaneously so that the overall time cost for exploring the region-of-interest is minimized. As a variation of the *Expanding Squares search* pattern, the *Expanding Spirals search* strategy was proposed in [36] to provide a more effective search with a shorter searching path. An energy-aware *Expanding Squares search* pattern is proposed to overcome the power constraint by optimizing the speed of each UAV while following the generated path in [37]. Again, the width between circles or squares is a critical factor for the final search result and is highly dependent on the sensor range of UAVs. Above all, the *Expanding Squares or Spirals* patterns are an exhaustive search, consistently resulting in a high exploration duration.

The *Grid-based search* pattern was proposed in [38] for a single UAV performing a target search mission. Later, it was extended to the cooperative search and rescue mission with a team of UAVs in [37,39]. The suggested method partitions the map into grid cells with equal size and then conducts the search of the target within each individual grid cell respectively, as shown in Fig. 2(d). The local search is performed by utilizing two of the aforementioned regular search patterns (*Creeping Line search* and *Expanding Squares search*) within each grid cell. From this aspect, it is also an exhaustive search procedure with high time costs and energy consumption. Besides, as discussed previously, the sensor capability of UAVs significantly affects the performance of local search within each grid cell. Some extensions have been made in [40–42] to reduce the search time by incorporating probability theory to eliminate the unnecessary search of less important grid cells. In [43], the power constraint is considered to enhance the efficiency of *Grid-based search* methods by introducing an energy-aware cost function. Whereas, the determination of the size of the grid cell requires a sound prior understanding of the search area. This constraint therefore, strongly limits the application of traditional *Grid-based search* in multi-UAV fire search missions in an unknown area. Our proposed search and survey technique modified the traditional *Grid-based search* method by reducing the dependency of prior information about the search area and UAVs' sensor capability from the perspective of grid partitioning. More importantly, we introduced a simple, yet effective local search pattern to conduct the exploration inside each grid cell.

### 3.2. UAV survey strategies for area estimation

The estimation for the area of fire zones is the second most important aspect of forest fire monitoring. Formation control has been used for multiple UAVs to discover the boundary of fire zones collaboratively in [14,17,27]. In [14,17] a simple ellipse was used to model the actual shape of the fire, and a group of UAVs were assigned to identify the boundary of the fire by following the perimeter of the ellipse. Another strategy proposed was for multiple UAVs to survey the border of the fire zone by dynamically changing the heading angle of UAVs [27]. Unlike [14,17], a circular fire model is used as the representation of the actual fire zone. Both of these two survey strategies utilized the leader-and-follower formation to identify the boundary of the fire through *dynamic formation control* (DFC). In [44], the footprint of the fire zones is assumed to be circular, and a distributed framework is proposed for multiple UAVs to survey the perimeter of the fire zone collaboratively. Fire zones normally have arbitrary shapes, and the assumption of an elliptical or circular fire model is ill-suited for most real-life scenarios.

## 4. Proposed methodology

In this section, a two-step search and survey procedure is proposed for a team of heterogeneous UAVs to perform the search and area estimation for forest fires. For clarity, we deconstruct our proposed multi-UAV system into two principal components: (i) the fire search procedure, and (ii) the fire boundary survey procedure. The details of each procedure are discussed below.

### 4.1. Search for fire zones

As mentioned in Section 3, grid-based search strategies have been widely used in many search and rescue missions for UAVs. In this paper, the proposed method utilizes a grid map for the search of potential fire zones. With $p$ available *sprint* UAVs, the search area $A$ is divided into $p$ equal square grid cells with area $A_c = \frac{A}{p}$. Then, all $p$ *sprint* UAVs are preplanned to conduct the search of the fire zones, and each *sprint* UAV is assigned with a specific grid cell, as shown in Fig. 3. At the same time, $q$ *survey* UAVs are send to the center of the grid cells for loitering so that they can be quickly switched to the boundary surveying operation

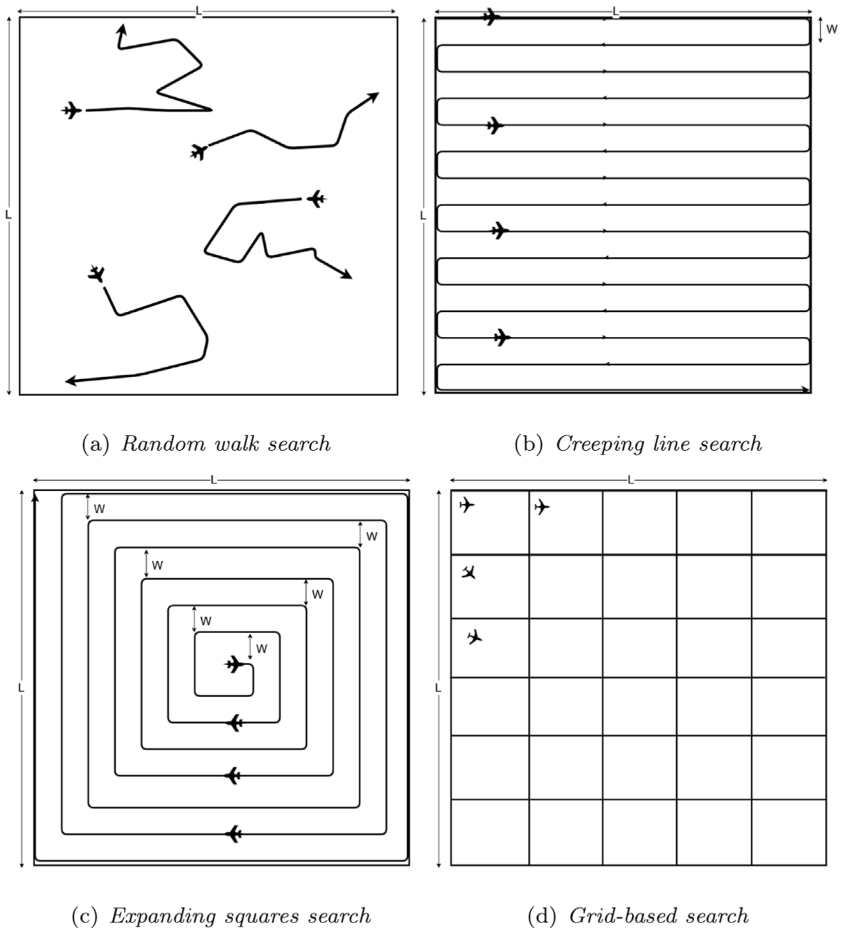


(a) *Random walk search* (b) *Creeping line search*

(c) *Expanding squares search* (d) *Grid-based search*

**Fig. 2.** Graphical description of several common search patterns.

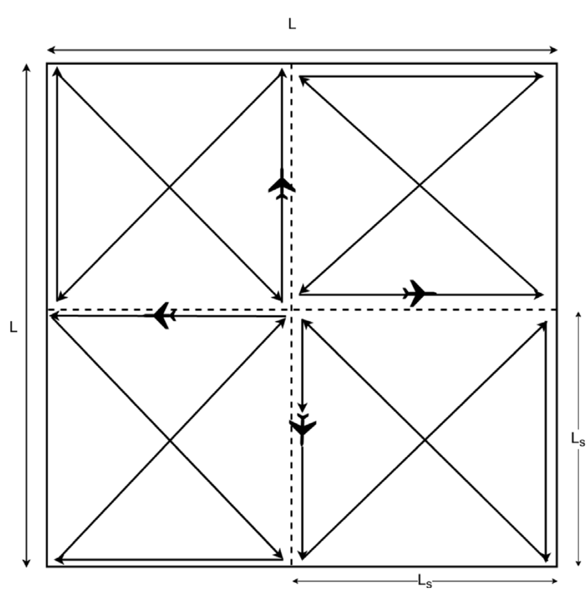


**Fig. 3.** Proposed search pattern. The dotted line shows the boundary of each grid cell.

for any neighboring detected fire zones. However, unlike other existing search paths, the proposed approach adopts a new search pattern for the local search within each grid cell. The shape of the proposed search pattern is similar to the 2*D* projection of a sand clock. It is because of this that is referred to as the *Sandclock* search pattern. As shown in Fig. 3, the *Sandclock* search pattern is rotated by $\frac{\pi}{2}$ radian in the neighboring grid cell to avoid repeating the search for fires in the boundary regions, improving the overall search efficiency. The generated trajectory of the *Sandclock* search pattern is a set of way-points (latitudes, longitudes, and altitudes). The altitude of a way-point has been calculated by adding a safe height (100 m in our implementation) according to the terrain information. The calculated safe altitude reduces the chance of potential collision of the UAVs within the terrain. Assuming that all the UAVs have a robust low-level controller capable of following the given way-points reliably.

Considering that real-world forest fires usually spread quickly and have a large impacted area after a short period of time, UAVs have a higher chance to detect the fire zone by following the *Sandclock* search pattern. Using elemental geometry arguments, from Fig. 3 it is seen that the *Sandclock* pattern guarantees the detection of an occurring fire zone if $a_{firezone} > \frac{A_c}{4}$, where $a_{firezone} \in \{a_1, a_2, \ldots, a_n\}$. This condition indicates that the proposed search pattern will go through the fire zone area when the fire zone covers a quarter of the grid cell. Although the initial area of the fire zones may not satisfy this condition, fire zones are constantly expanding (over time) and their area increases accordingly, which will result in rapidly meet this condition.

To show the benefits of the proposed search pattern, we compare it with two standard search patterns, specifically, the *Creeping Line search* and the *Expanding Squares search*. Let $L$ be the length of the entire search area and $L_s$ be the length of each grid cell such that $L = \sqrt{A}$ and $L_s = \sqrt{A_c}$ where we have assumed a

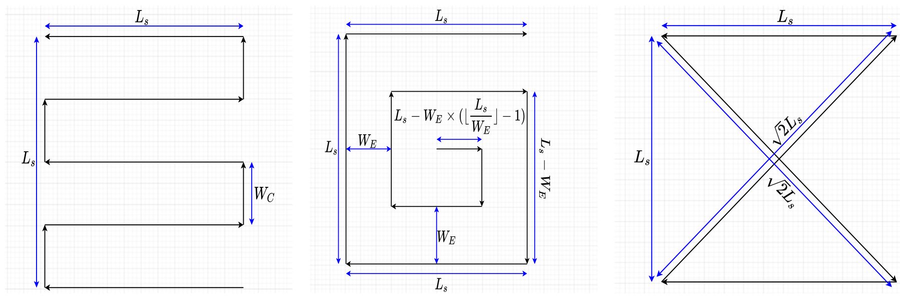


(a) *Creeping line* (b) *Expanding squares* (c) *Sandclock*

**Fig. 4.** Graphical representation of the *Creeping Line* (CL-search), *Expanding Squares* (ES-search) and the proposed *Sandclock* search patterns within each grid cell.

square search area. Below, we compare the path lengths of three search patterns.

*Creeping Line search* (CL-search): As shown in Fig. 4(a), let $W_C$ be the width between two consecutive line segments; it is easy to show that there are $\lfloor \frac{L_s}{W_C} \rfloor + 1$ horizontal lines and $\lfloor \frac{L_s}{W_C} \rfloor$ vertical segments of length $W_C$ within each grid cell. Thus, the total length $L_{T_C}$ of the *Creeping Line* search pattern is calculated as:

$$L_{T_C} = L_s \times \left( \left\lfloor \frac{L_s}{W_C} \right\rfloor + 1 \right) + \left\lfloor \frac{L_s}{W_C} \right\rfloor \times W_C = \frac{L_s^2}{W_C} + 2L_s. \tag{1}$$

*Expanding Squares search* (ES-search): In Fig. 4(b), let $W_E$ be the fixed width by which each square increases; then, $\lfloor \frac{L_s}{W_E} \rfloor$ squares are generated within a grid cell. The length of the outermost square can be expressed as $3L_s$. The next inner square has a of length $2\,(L_s - W_E)$ and the length of the innermost square is $2\left( L_s - W_E \times \left( \left\lfloor \frac{L_s}{W_E} \right\rfloor - 1 \right) \right)$. Therefore, the overall length $L_{T_E}$ of the *Expanding Square* search is written as below:

$$\begin{aligned} L_{T_E} &= 3L_s + 2 \sum_{i=1}^{\lfloor \frac{L_s}{W_E} \rfloor - 1} (L_s - W_E \times i) \\ &= 3L_s + 2 \sum_{i=1}^{\lfloor \frac{L_s}{W_E} \rfloor - 1} L_s - 2W_E \times \sum_{i=1}^{\lfloor \frac{L_s}{W_E} \rfloor - 1} i \\ &= 3L_s + 2L_s \times \left( \left\lfloor \frac{L_s}{W_E} \right\rfloor - 1 \right) - 2W_E \times \frac{\left( \left\lfloor \frac{L_s}{W_E} \right\rfloor - 1 \right) \times \left\lfloor \frac{L_s}{W_E} \right\rfloor}{2} \\ &= 3L_s + 2\frac{L_s^2}{W_E} - 2L_s - \frac{L_s^2}{W_E} + L_s \\ &= \frac{L_s^2}{W_E} + 2L_s. \end{aligned} \tag{2}$$

*Sandclock search*: In Fig. 4(c), the proposed search pattern does not perform any further decomposition inside the grid cell, and it searches the space by following a path similar to the shape of a Sandclock. Thus, the total length $L_{T_P}$ of the proposed search pattern becomes:

$$L_{T_P} = L_s + \sqrt{2}L_s + L_s + \sqrt{2}L_s = \left(2 + 2\sqrt{2}\right) \times L_s. \tag{3}$$

From Eq. (3), the size of the grid cell $L_s$ can be derived as $L_s = \frac{L_{T_P}}{2+2\sqrt{2}}$. By substituting $L_s$ in Eqs. (1) and (2) we get the following equations:

$$L_{T_C} = \frac{L_{T_P}^2}{(2+\sqrt{2})^2 W_C} + \frac{2L_{T_P}}{2+2\sqrt{2}}, \tag{4}$$

and

$$L_{T_E} = \frac{L_{T_P}^2}{(2+\sqrt{2})^2 W_E} + \frac{2L_{T_P}}{2+2\sqrt{2}}. \tag{5}$$

From Eq. (4), there is a quadratic relationship between $L_{T_C}$ and $L_{T_P}$ when $W_C$ is fixed. With a fixed value of $W_E$, Eq. (5) shows that the overall length of the ES-search increases quadratically as the length of the proposed search pattern increases. From this aspect, the total travel distance of the proposed search pattern is smaller than the CL-search and ES-search patterns. To further compare the overall travel distances among these three search patterns, the following equations are obtained:

$$L_{T_P} > L_{T_C}, \text{ if, } \frac{L_s}{W_C} < 2\sqrt{2}, \tag{6}$$

$$L_{T_P} > L_{T_E}, \text{ if, } \frac{L_s}{W_E} < 2\sqrt{2}. \tag{7}$$

In Eqs. (6) and (7), the proposed search pattern shows longer travel distance when the ratio between the size of the grid cell and the width between lines or squares falls below $2\sqrt{2}$. This condition means that the number of lines or squares needs to be less than three (3), and a small grid cell is required. Accordingly, the total number of grid cells increases and more UAVs are required to complete the search task, significantly increasing the search cost. Therefore, the proposed search pattern is more efficient than the other two search patterns (CL-search and ES-search).

The search coverage area for three search patterns has been calculated using the specification of fire detection sensors. The entire search area $A$ is partitioned into smaller grid cells of area $b \times b$ (area of the fire detection sensor's footprint). The central node assigns a value to each cell according to Eq. (8). If $n$ is the number of all captured cells by the sensor, then at the end of the mission the total coverage area will be $A_{cov} = n \times b \times b$. The impact of the size of the covered area is discussed in Section 6.

$$cell_{i,j} = \begin{cases} 1, & \text{if a UAV is inside the cell;} \\ 0, & \text{otherwise.} \end{cases} \tag{8}$$

### *4.2. Fire boundary survey strategy*

After locating the fire zone, the next task for the UAVs is to survey the fire zone and estimate its area. Multiple UAVs are used to survey one fire zone. The UAV which found the fire zone will share its location with the rest of the UAVs in the system. A subgroup of $m$ ($m < q$) closest UAVs will fly to the location of the source and loiter around until the fire zone is identified, due to its increasing size and perceptual shift in location. If this subgroup of UAVs detect the existence of fire around that location, they begin the survey phase of the monitoring process. Once the group of surveying units is informed about the location of a fire zone heading towards it, they may then discover another one. The detected fire boundary points are stored in a central database as a unified list, irrespective of which point belongs to which fire zone. To this end, a clustering algorithm is applied before estimating the area of a fire zone, as discussed in Section 4.3.

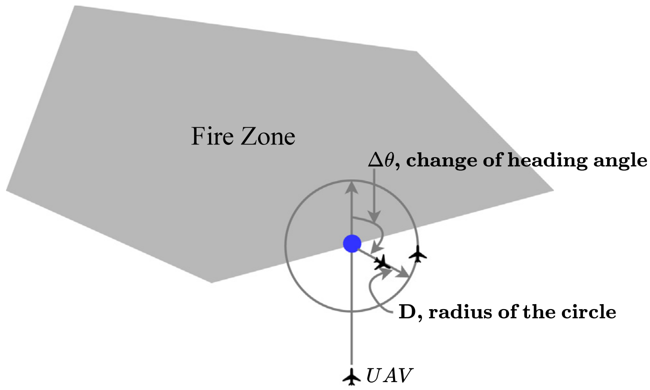


**Fig. 5.** Survey procedure.

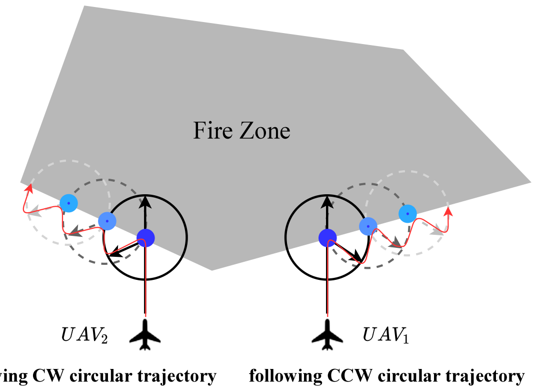


**Fig. 6.** Continuation of the survey procedure for two *UAVs*. The red lines are the trajectories of the two *UAVs* during the survey procedure.

The value of $m$ depends on the availability of the UAVs. In the simulation, we called only from the $q$ *survey* UAVs while the *sprint* UAVs will continue to explore the other areas in the search region. To survey the fire boundary, we developed a new strategy as shown in Fig. 5. Besides, there is the risk of losing a UAV when it hovers more than $\Delta t$ seconds on top of the fire zone. This constraint is considered in the proposed survey strategy. In Fig. 5, we denote by $\Delta\Theta$ the change of heading angle when the UAV identifies the existence of a fire boundary point from the fire detection sensor. The UAV may enter into the fire zone because of its inertial motion. The angle $\Delta\Theta$ can be tuned to reduce the time of stay on top of a fire zone. Smaller $\Delta\Theta$ will increase the time of stay and larger $\Delta\Theta$ reduces the time of stay. Because the shape of the fire zone is an irregular polygon, there is not a closed-form expression of the time of stay as a function of $\Delta\Theta$.

The blue dot in Fig. 5 is the detected boundary point by the UAV. Since multiple UAVs survey the same fire zone, two consecutive UAVs follow the circle in two different directions. The first UAV surveys the fire zone by following the circular trajectory clockwise, while the second UAV will follow the circular trajectory counterclockwise (if it gets the fire source location from the first UAV) as illustrated in Fig. 6. This directional approach restricts two consecutive UAVs to explore same boundary points if they are surveying the same fire zone. In the proposed survey procedure, $D$ is considered as a safe distance, and it is included as a design parameter. If $D$ is large, then the sampled points from the fire boundary will be far from each other, whereby for a smaller $D$ the sampled points will be closer to each other. As such, the safe distance, $D$, will affect the final estimation of the fire zones' shape. As shown in Fig. 6, a UAV could successfully survey the whole fire zone by following these cycles. Algorithm 1 summarizes UAV's survey procedure.

**Algorithm 1:** Survey algorithm

**Input**: $D$, $\Delta\theta$, *direction*
$\gamma$ = reading from the fire detection sensor;
**while** *Simulation running* **do**
    Change the heading angle of the UAV by $\Delta\theta$;
    $C$ = Currently detected fire boundary point;
    /* This is the position of the UAV while fire detection sensor detects fire and $\gamma$ is True. */
    **if** *direction* == *clockwise* **then**
        $\tau$ =
        A CW circular trajectory with center at $C$ and radius $D$;
    **else**
        $\tau$ =
        A CCW circular trajectory with center at $C$ and radius $D$;
    **end**
    Send trajectory $\tau$ to the UAV;
    /* The UAV is assumed to follow the trajectory unless new command is sent to it. */
    **while** $\gamma$==*False* **do**
        Wait;
    **end**
**end**
/* A CW circular trajectory indicates that the UAV will follow the circle in a clockwise direction and for CCW, the UAV will follow the circle in a counter clockwise direction as shown in Fig. 6. The terrain of area $A$ is used to calculate the way-points of all the trajectories as described in Section 4.1. */

*4.3. Estimation of the fire zone area*

In this research, multiple UAVs are used to conduct the search and survey tasks for fire zones and one fire zone can be surveyed by more than one UAV. From the survey procedure, a collection of 2D sampled points are obtained and these sampled points are used to conduct the area estimation for fire zones. In Fig. 7, $fz_1$ is being surveyed by $UAV_1$ and $UAV_3$. The blue dots are the sampled boundary points of the fire zone from the corresponding UAVs in Fig. 7. We stored all the sampled points in a central database and a grouping algorithm is required for selecting the boundary points of a particular fire zone. For grouping the corresponding fire zone boundary points, we used the Mean-Shift Clustering algorithm. Unlike most of the existing clustering approaches, the mean-shift clustering method introduces the multivariate kernel density estimator to approximate the density distribution of the data and then extracts the cluster structure using the estimated density distribution. An overview of the Mean-Shift Clustering algorithm is summarized in algorithm 2 and details can be found in [45,46].

**Algorithm 2:** Mean-Shift clustering algorithm

Select the kernel function;
Estimate the bandwidth of the kernel function;
**while** *The estimated density distribution is not converged* **do**
    Compute the mean-shift vector using gradient descent;
    Update the kernel function using the mean-shift vector;
    Estimate the density distribution with the kernel function;
**end**
Identify the mode of the estimated density distributions as the clusters;

Compared with the state-of-the-art clustering approaches, the Mean-Shift Clustering algorithm is able to group the input data points without knowing the true number of clusters. Since the number of fire zones is unknown, the Mean-Shift Clustering algorithm is a suitable choice for the problem presented. Moreover, the Mean-Shift Clustering showed a strong robustness to the noises, or outliers, which may address potential data corruption in multi-UAVs fire search and survey missions. More importantly, the mean-shift clustering has been recently used for information processing in UAV-based sensing missions and has shown promisingly good performance [47]. The latitude, $X$, and longitude, $Y$, of the sampled points are used as the primary feature representation for the subsequent data clustering analysis. Let $P = \{X, Y\}$ be the coordinates of a sampled point $i$; the set of all sampled points is denoted as $P_s = \{P_i | i = 1, 2, \ldots, |P_s|\}$. The Mean-Shift Clustering algorithm takes the set $P_s$ as the input to perform the cluster analysis. With the clustering procedure, all sampled points are grouped into a set of clusters $C = \{C_i | i = 1, 2, \ldots, |C|\}$, where $C_i = \{P_j^{C_i}, j = 1, 2, \ldots, |C_i|\}$. Each cluster of sample points captures the shape of the fire zones' boundary and the area of the fire zone is estimated by connecting the boundary points sequentially within each cluster. Every two consecutive boundary points from cluster $C_i$ can be connected with different types of curves. In our implementation we used a straight line to connect them. The area of the fire zone is calculated using fundamental image processing techniques. Specifically, a polygon with the sampled boundary points is drawn inside a black background image with height $h$ and width $w$. Then, the polygon is filled with white pixels. The area is calculated by counting the number of white pixels in the image. Using the same width and height, another image is created for the true polygon. A bitwise *AND* operation is conducted on the two images to calculate the intersection area of the estimated fire zone and true fire zone. To measure the efficacy of the survey algorithm, we calculate the Intersection Over Union ($IOU$) using the true polygon area and the estimated polygon area. Let $A_1$ be the true area of a fire zone, $A_2$ the estimated area, and $A_3$ the intersection area of $A_1$ and $A_2$. Then, the $IOU$ can be calculated as $IOU = \frac{|A_1 \cap A_2|}{|A_1 \cup A_2|} = \frac{|A_3|}{|A_1|+|A_2|-|A_3|}$. The $IOU$ value is between zero and one, where a value of one indicates perfect estimation of the fire zone area and zero means the estimated area is completely outside of the true area.

The fire zone can expand, shrink, and translate over time in space due to the wind impact. Therefore, we adjust the estimated area of the fire zone based on wind speed and direction in each time stamp. The wind speed and direction can be directly obtained from the on-board sensor of the UAV. All the sampled fire boundary points are updated by wind speed and direction according to

$$\begin{aligned} X_{new} &= X_{old} + v_w \cos\theta_w, \\ Y_{new} &= Y_{old} + v_w \sin\theta_w, \end{aligned} \tag{9}$$

where $X$ and $Y$ are the temporal coordinate of the fire boundary point, $v_w$ is the wind speed, and $\theta_w$ is the wind direction with respect to the Geodetic coordinate system.

## 5. Experimental setting

In this section, we describe the simulation software and the simulation scenarios that have been used to develop our method and test its performance. We also discuss the selection criteria of the various user-defined parameters of our approach.

### 5.1. Simulation software

The AMASE [20] was developed by the Air Force Research Laboratory (AFRL); it is a simulation platform for the analysis of multi-agent unmanned aerial systems. It is written in Java programming language and has a graphical user interface, which allows the users to keep track of the simultaneous behavior of multiple UAVs. The simulation data can be directly saved and exported for post-analysis from the simulation software. In addition, a playback tool is developed to retrieve the scenario events after finishing a simulation in AMASE. The search and survey algorithm can be implemented using Java, C++, or Python programming language, which works as a client to the AMASE simulator. Specifically, the AMASE simulator creates a server which can be accessed through a client software. The data among the AMASE server and other clients are exchanged using the User Datagram Protocol (UDP). Different simulation scenarios are developed using simple Extensible Markup Language (XML). Events such as the fire zone boundary, the UAV configuration, the search boundary and the UAV states can be described using appropriate tags in the XML file.

### 5.2. UAVs' navigation, coordination and control in AMASE

The common mission automation services interface (CMASI) is used to develop the navigation, coordination and control system of the UAVs in AMASE [48]. The autonomous capabilities and payloads of the UAV can be described using CMASI data structure. The **AirVehicleConfiguration** structure is defined in CMASI to include information regarding the kinematic capabilities of the UAV, and contains a list of objects that describe the individual payload items that are on the UAV. A list of **FlightProfile** structures is defined to describe the kinematic capabilities of a UAV. Each **FlightProfile** contains information regarding speed, maximum bank angle, fuel consumption, and climb (or descent) rate for a given condition. An **AirVehicleConfiguration** can have more than one **FlightProfile** to execute different actions such as cruise, dash, loiter, climb or descent. CMASI defines three payload types named as **CameraConfiguration**, **GimbalConfiguration**, and **VideoStreamConfiguration**. CMASI includes an **AirVehicleState** structure that is updated periodically during the simulation. The **AirVehicleState** contains the position, orientation, and velocity data of the UAV, as well as the energy remaining. To control each UAV, two types of action commands can be sent to the UAVs in AMASE, categorized as Navigational and Payload action. CMASI provides two data structure for issuing one of these action commands. One of them is **VehicleActionCommand** and the other is **MissionCommand**. The **VehicleActionCommand** is used to execute basically a payload command such as steering a gimbal. The **MissionCommand** is used to execute waypoint navigation. The waypoints are formed as a linked list. Each waypoint contains the speed, climb rate, turn type (fly-past, or turn-short) as well as a contingency point that may be used by the UAV in the case of an emergency (e.g. lost communications). In our implementation, we employ the **MissionCommand** structure. The Central node generates appropriate waypoints for each UAV in the system and sends them to the UAV. In a repeated feedback loop, the central node observes whether each UAV has finished the mission or not and takes actions accordingly, for instance the generation of the next set of waypoints as described in Sections 4.1 and 4.2.

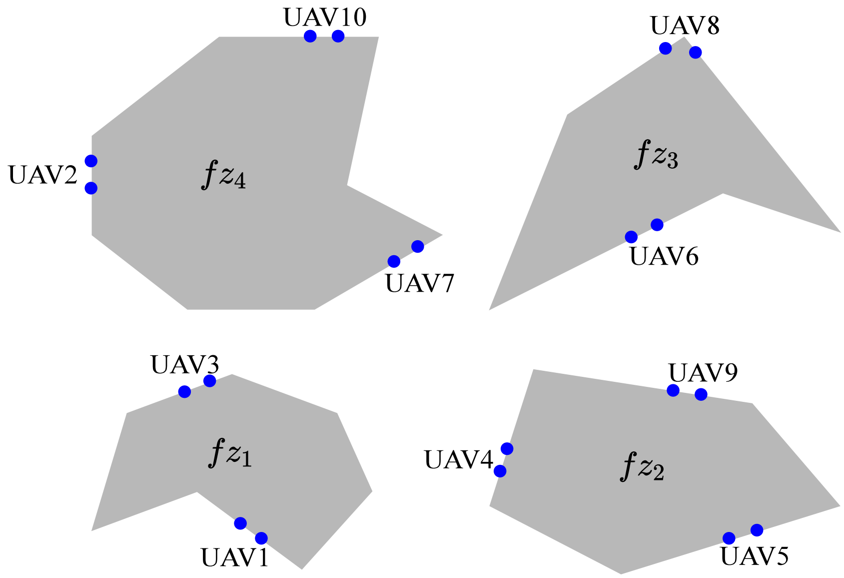


**Fig. 7.** A sample scenario while multiple UAVs are surveying multiple fire zones.

### 5.3. Scenarios description

In order to evaluate the efficacy of the proposed two-step search and survey strategy, forty-five scenarios from the *Swarm Search AI Competition: Fire Hack 2019*[1] [49] are used in the simulation. Each scenario has a one-hour default simulation duration which we extend to ninety minutes in the experiments. It starts with the simplest scenario and gradually increases the complexity of the simulation scenarios. These simulation scenarios are designed based on real-world constraints [49], determined by experts from AFRL. The details are summarized below:

- Multiple fire zones exist in different locations simultaneously and the fire zones move, expand and shrink over time.
- Two different types of UAVs, defined as the *Sprint* UAVs and the *Survey* UAVs, are used in the simulation.
- The topography of the search area is considered in each scenario and UAVs flyly safe over the landscape of area $A$.
- *Sprint* UAVs have limited power for searching.
- UAVs will crash and be lost if they stay more than 10 seconds over fire zones, or out of the search region.

We categorize the forty-five scenarios into three primary types, *Type-I*, *Type-II*, and *Type-III* scenarios. The specifications of these three types of scenarios are summarized in Table 1. The difference among different scenarios of a particular type is the initial location of the UAVs, the initial location of the fire zones, and the shape of the fire zones. All these parameters, including the initial locations of UAVs as well as fire zones, and the shape of fire zones, are drawn from a uniform distribution. The UAVs and fire zones are placed inside the search area randomly, while UAVs or fire zones are not allowed to be placed in the same geographical location inside $A$. The random placement of UAVs and fire zones ensures that the scenarios are not biased to any particular search pattern.

### 5.4. Parameter setting

As described in Section 4.2, several parameters need to be specified for the survey operation. According to the default setting in [20] and predefined parameters from [49]; the overall simulation duration, size of the search region, maximum hovering time for UAV above fires, and the characteristics of the UAV types are summarized in Table 2. The values of the safe distance and change in heading angles are specified in Table 2 as well. Considering the maximum speed of the *survey* UAVs, the safe distance is set to be 500 meters giving UAVs a flying time of twenty seconds away from the fires. The change in heading angle is set as 2.827 rad to guarantee a small probability of crash for the UAV. During the search operation the *sprint* UAVs are flying at a constant velocity of 35 m/s, and during the survey operation both types of UAVs are flying at 20 m/s. For all scenarios, the same parameter setting is used for the UAVs at the survey mode.

## 6. Experiments and result discussions

In this section, the proposed search and survey technique is implemented on the AMASE simulator and its efficacy is evaluated based on two metrics: (a) search performance, and (b) survey performance. The simulation results are discussed in the following subsections.

### 6.1. Search performance

In order to justify the search efficacy of the proposed search pattern, all three search patterns – CL-search, ES-search, and *Sandclock*-search – are simulated herein, and a comparison study is conducted. According to Tables 1 and 2, we can calculate the total travel distance required for the three search patterns using Eq. (1), (2), and (3). The total travel distances are listed in Table 3. From Table 3, it is clear that the proposed search pattern required comparably less travel distance than the other two patterns. Further, to show the efficacy of the proposed search pattern, we used all forty-five scenarios for all three types defined and took the average search performance for comparison. For each search pattern, the overall detection time of all fire zones and the search coverage area in the same scenario are obtained. The average of the overall detection time and the search coverage area are computed across each scenario type. With the averaged fire detection time and search coverage area, the comparison results are presented in Table 4. For CL-search and ES-search, the value of $W_C$ or $W_E$ is set to be 2628.02 m, 5256.03 m, and 13140.09 m,

[1] The proposed approach has been applied in real-time to the competition scenarios and the authors secured 2nd place in the Final showcase held in Dayton, OH, 2019.

**Table 1**
The summary of all forty-five scenarios in terms of the number of fire zones, power constraints, sudden crash of UAVs, and number of *sprint* and *survey* UAVs.

| Scenario type | Scenario specifications | No. of scenarios |
|---|---|---|
| *Type-I Scenarios*: | Two fire zones; No power constraint;<br>Two fire zones; No power constraint; 6 *sprint* + 2 *survey* UAVs; No sudden crash of UAVs | 15 |
| *Type-II Scenarios:* | Three fire zones; Power constraint;<br>6 *sprint* + 3 *survey* UAVs; No sudden crash of UAVs | 15 |
| *Type-III Scenarios:* | Three fire zones; Power constraint;<br>6 *sprint* + 4 *survey* UAVs; Sudden crash of UAVs | 15 |

**Table 2**
Parameters setting.

| | |
|---|---|
| The Overall Simulation Duration ($T$) | 5400 s |
| Change of Heading Angle ($\Delta\Theta$) | 2.827 rad |
| Safe surveying distance for UAVs (D) | 500 m |
| The Entire Search Area ($A$) | 64373 × 64373 m$^2$ |
| Length/Width of the Entire Search Area ($L$) | 64373 m |
| Max. hovering time of a UAV above a fire zone or out of search boundary ($\Delta t$) | 10 s |
| Footprint of the fire detection sensor ($b \times b$) | 10 × 10 m$^2$ |
| Max. speed of the *sprint* UAVs ($v_{sp}$) | 35 m/s |
| Max. sensor detection range of the *sprint* UAVs ($R_{sp}$) | 500 m |
| Max. speed of the *survey* UAVs ($v_{su}$) | 25 m/s |
| Max. sensor detection distance of the *survey* UAVs ($R_{sp}$) | 1000 m |

**Table 3**
Total travel distance for the three search patterns. Here, $L = 64373$ m, $p = 6$, $Ls = \frac{L}{\sqrt{p}} = 26280.17$ m and $W_C = W_E = 2628.02$ m.

| | CL-search ($L_{T_C}$) | ES-search ($L_{T_E}$) | Sandclock search ($L_{T_P}$) |
|---|---|---|---|
| Total travel distance | 315.36 km | 315.36 km | 126.89 km |

**Table 4**
Comparison of *Creeping line* and *Expanding square* search patterns with the proposed *Sandclock* search pattern for three types of scenarios. The results are averaged over fifteen scenarios of each type.

| | *Type-I* | | *Type-II* | | *Type-III* | |
|---|---|---|---|---|---|---|
| | $A_{cov}$ (km$^2$) | Time (s) | $A_{cov}$ (km$^2$) | Time (s) | $A_{cov}$ (km$^2$) | Time (s) |
| CL-search $W_C = 2628.02$ | 446.23 | 1912.7 | 428.73 | 1868.37 | 498.6 | 2088.89 |
| CL-search $W_C = 5256.03$ | 427.64 | 1488.32 | 431.36 | 1677.25 | 465.92 | 1990.27 |
| CL-search $W_C = 13140.09$ | 387.17 | 1780.36 | 396.55 | 2147.49 | 474.47 | 2492.73 |
| ES-search $W_E = 2628.02$ | 420.78 | 1751.67 | 398.6 | 1909.26 | 492.74 | 2189.07 |
| ES-search $W_E = 5256.03$ | 389.72 | 2253.1 | 423.17 | 1995.15 | 479.52 | 2349.2 |
| ES-search $W_E = 13140.09$ | 389.92 | 2187.69 | 430.73 | 1854.21 | 469.84 | 2216.58 |
| Sandclock search | 374.37 | **930.04** | 437.37 | **1264.13** | 499.56 | **1896.04** |

respectively. Fig. 8 shows the implementation of all three search patterns in the AMASE simulator.

In terms of the average detection time, Table 4 demonstrates that the proposed search pattern is always faster than the other two compared search patterns in all three groups of scenarios. In the *Type-I* and *Type-III scenarios*, the CL-search takes the longest average time to detect all fire zones and the ES-search pattern has the second shortest average detection time. However, the CL-search achieves a faster detection of fires than the ES-search in the *Type-II scenarios*. The average detection time of the CL-search and ES-search patterns directly depends on the value of $W_E$ and $W_C$. For the average search coverage area, it is observed that the *Sandclock* search covers less area in *Type-I scenarios* due to the unlimited power. Conversely, the *Sandclock* shows higher search coverage area than the other two compared search patterns in *Type-II* and *Type-III scenarios*. Since these two types of scenarios assume UAVs have limited power, the *Sandclock* search finishes the search of a grid cell with shorter travel path and it is more likely to explore more cells with limited power during the search procedure. In contrast, the other two search patterns take longer travel distance to scan the cell with less chance to visit other cells. As the complexity of the scenario increases, Table 4 reveals that the proposed search pattern always shows the fastest average detection time of fire zones while the performance of the CL-search and ES-search change dramatically. Therefore, it is clear that the proposed search pattern consistently shows better performance in the detection of fire zones than the other two search patterns as the scenarios change.

### *6.2. Survey performance*

As discussed above, the proposed search procedure shows better performance than the other two well-known search patterns. To show the survey performance of the proposed approach,

**Table 5**
The summary of simulation results on all forty-five scenarios in terms of the number of the detected fire zones, average *IOU* of the estimated fire zones, and number of crashes (topography, fires, or insufficient fuel level).

| Scenario | Performance | 60 min | 90 min |
|---|---|---|---|
| *Type-I Scenarios*: | No. of fires:<br>*IOU*:<br>No. of crashes: | 2<br>(0.79, 0.88)<br>0 | 2<br>(0.95, 0.99)<br>0 |
| *Type-II Scenarios:* | No. of fires:<br>*IOU*:<br>No. of crashes: | 3<br>(0.75, 0.90, 0.96)<br>1 | 3<br>(0.94, 0.96, 0.98)<br>1 |
| *Type-III Scenarios:* | No. of fires:<br>*IOU*:<br>No. of crashes: | 3<br>(0.63, 0.86, 0.90)<br>1 | 3<br>(0.86, 0.95, 0.98)<br>1 |

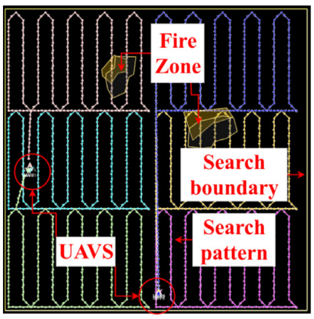


(a) *Creeping line*

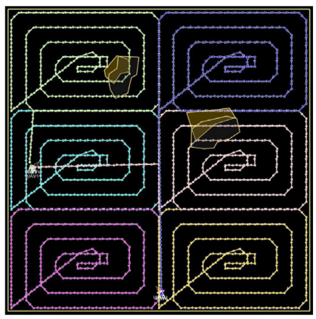

(b) *Expanding squares*

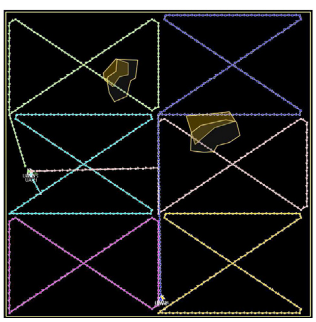

(c) *Sandclock*

**Fig. 8.** Implementation of different search patterns in simulation (one of forty-five scenarios).

experiments are conducted on all three types of scenarios. In each scenario, the IOU estimation of each fire zone are reported at $t = 60$ *mins* and $t = 90$ *mins*, serving as the evaluation measure for the survey performance. Based on the IOU estimation, we provide a detailed discussion on the *Type-I Scenarios*. A summary for the results of the remaining scenarios is presented in Table 5.

From Table 5, it is observed that the proposed search and survey method successfully discovers all fire zones and performs a good area estimation for the *Type-I scenario*. The estimated IOUs for fire zones are 0.7904 and 0.9410 within sixty minutes, respectively. After ninety minutes, the estimated IOU values are close to one, which indicates that the proposed technique accurately estimates the area of all fire zones. Similar to the *Type-I scenarios*, the proposed technique also captures all fire zones and achieves an accurate area estimation for fire zones for the remaining two groups of scenarios, which is shown in Table 5. Specifically, all fire zones are discovered within sixty minutes and the estimated IOUs are above 0.8, which implies the efficacy of the proposed search and survey technique. The overall ninety-minutes IOU estimation further implies that the proposed technique guarantees to effectively identify the boundary of fire zones and provide a more accurate area estimation if sufficient time is given. Further, Table 5 reveals that the proposed technique leads to a small number of crashes for UAVs when the complexity of scenarios increases.

### 6.3. Summary of discussions

Based on the search and survey performance, the following observations can be summarized:

1. The proposed search pattern could always provide a faster search of fire zones than other two search patterns as the complexity of the simulation scenario increases.
2. The proposed survey strategy effectively discovers the boundary of fire zones and provides an accurate coverage estimation of fire zones. It also reduces the chance for the loss of UAVs by avoiding the long time stay over fires while surveying the boundary of fire zones.
3. The proposed search and survey technique improves the accuracy of the area estimation for fire zones by considering the effect of the wind and utilizing the mean-shift clustering technique.

Therefore, we can conclude that the proposed two-step search and survey technique not only achieves the earliest detection of fire zones, but also provides an accurate estimation for the area of fire zones.

## 7. Conclusion

In this paper, a two-step search and survey procedure is presented for a group of UAVs to discover possible wildfires and provide accurate area estimations of fire zones. In the search stage of fire zones, an original search pattern, namely the *Sandclock* pattern, is developed to perform a fast scan within each individual grid cell. Compared with the CL-search and ES-search patterns, the *sandclock* search pattern has a relatively shorter path, which is more realistic for application to real-world systems. A theoretical comparison and related explanations are provided to support the efficiency of the proposed search pattern. In the survey procedure, an effective strategy is introduced for multiple UAVs to effectively identify the boundary of the fire zone, and provided an accurate estimation of its area. The proposed survey technique is able to reduce the possibility for UAVs to stay in the fire zone for a long time and it could successfully alleviate the crash of UAVs in the fire zones. The mean-shift clustering technique is used to merge highly overlapped small fire zones in the data analysis procedure and deliver an accurate estimation for the overall areas of fire zones.

Based on the comparison results with the other two popular search patterns, the *sandclock* search shows a better performance in the search procedure and it is less sensitive to rapid environmental changes in the scenarios. In the survey stage, simulation results reveals that the proposed survey technique leads to a high-quality survey performance. The simulation results demonstrate that the proposed search and survey technique could successfully discover the fire zones within a short time and provide an accurate area estimation for the fire zones. Additionally, the presented search and survey technique is not limited to wildfires detection. It can be easily extended to monitor other natural disasters and border security applications such as flooding, earthquakes, border patrol and epidemic spread of diseases.

In the future, the extension of the proposed search and survey technique will be conducted to enhance the performance of multi-agent systems in other search and rescue events.

## Declaration of competing interest

The authors declare that they have no known competing financial interests or personal relationships that could have appeared to influence the work reported in this paper.

## Acknowledgments

The authors would like to thank TECHLAV, United States of America for the financial support under the agreement number FA8750-15-2-0116 and the U.S. Air Force Research Laboratory for allowing to use their AMASE software before, during and after the "Swarm and Search AI Challenge: 2019 Fire Hack" event, which was hosted by the Wright Brothers Institute and University of Dayton Research Institute. Also, this work is partially funded through the National Institute of Aerospace's Langley Distinguished Professor Program, United States of America under grant number C16-2B00-NCAT. The authors would also like to thank the NASA Langley Research Center, United States of America and the NASA University Leadership Initiative (ULI), United States of America under agreement number 2 CFR 200.514.

## Appendix A. Supplementary data

Supplementary material related to this article can be found online at https://doi.org/10.1016/j.robot.2021.103848.

## References

[1] M. Kumar, K. Cohen, B. HomChaudhuri, Cooperative control of multiple uninhabited aerial vehicles for monitoring and fighting wildfires, J. Aerosp. Comput. Inf. Commun. 8 (1) (2011) 1–16.
[2] D. Jergler, Carr fire losses may reach $1.5B in likely another destructive season for California, Insur. J. (2018).
[3] C. Nugent, Camp fire death toll lowered after human remains were mistakenly sorted into separate bags, Time (2018).
[4] K. Mendes, Brazillan Amazon fires scientifically linked to 2019 deforestation: report, Mongabay Ser. (2019).
[5] British Broadcasting Corporation News, Australia Fires: A visual guide to the bushfire crisis, 2020.
[6] V.G. Ambrosia, S.S. Wegener, D.V. Sullivan, S.W. Buechel, S.E. Dunagan, J.A. Brass, J. Stoneburner, S.M. Schoenung, Demonstrating UAV-acquired real-time thermal data over fires, Photogramm. Eng. Remote Sens. 69 (4) (2003) 391–402.
[7] V.G. Ambrosia, S. Wegener, T. Zajkowski, D. Sullivan, S. Buechel, F. Enomoto, B. Lobitz, S. Johan, J. Brass, E. Hinkley, The Ikhana unmanned airborne system (UAS) western states fire imaging missions: from concept to reality (2006–2010), Geocarto Int. 26 (2) (2011) 85–101.
[8] C.C. Wilson, J.B. Davis, Forest Fire Laboratory at Riverside and Fire Research in California: Past, Present, and Future, Gen. Tech. Rep. PSW-105, Pacific Southwest Research Station, Forest Service, US Department of Agriculture. 22, Berkeley, Calif., 1988, p. 105.
[9] V.G. Ambrosia, T. Zajkowski, Selection of appropriate class UAS/sensors to support fire monitoring: experiences in the United States, Handb. Unmanned Aer. Veh. (2015) 2723–2754.
[10] M. Tranchitella, S. Fujikawa, T.L. Ng, D. Yoel, D. Tatum, P. Roy, C. Mazel, S. Herwitz, E. Hinkley, Using tactical unmanned aerial systems to monitor and map wildfires, in: AIAA Infotech@ Aerospace 2007 Conference and Exhibit, 2006, p. 2749.
[11] A. Restas, Wildfire management supported by uav based air reconnaissance: Experiments and results at the szendro fire department, Hungary, in: First International Workshop on Fire Management, 2006.
[12] R. Charvat, R. Ozburn, S. Bushong, K. Cohen, M. Kumar, SIERRA Team flight of Zephyr UAS at West Virginia Wild Land fire burn, in: Infotech@ Aerospace 2012, 2012, p. 2544.
[13] G.P.J. IV, L.G. Pearlstine, H.F. Percival, An assessment of small unmanned aerial vehicles for wildlife research, Wildl. Soc. Bull. 34 (3) (2006) 750–758.
[14] K.A. Ghamry, M.A. Kamel, Y. Zhang, Cooperative forest monitoring and fire detection using a team of UAVs-UGVs, in: 2016 International Conference on Unmanned Aircraft Systems (ICUAS), IEEE, 2016, pp. 1206–1211.
[15] C. Yuan, Y. Zhang, Z. Liu, A survey on technologies for automatic forest fire monitoring, detection, and fighting using unmanned aerial vehicles and remote sensing techniques, Can. J. Forest Res. 45 (7) (2015) 783–792.
[16] C. Phan, H.H. Liu, A cooperative UAV/UGV platform for wildfire detection and fighting, in: 2008 Asia Simulation Conference-7th International Conference on System Simulation and Scientific Computing, IEEE, 2008, pp. 494–498.
[17] K.A. Ghamry, Y. Zhang, Cooperative control of multiple UAVs for forest fire monitoring and detection, in: 2016 12th IEEE/ASME International Conference on Mechatronic and Embedded Systems and Applications (MESA), IEEE, 2016, pp. 1–6.
[18] K.A. Ghamry, Y. Zhang, Fault-tolerant cooperative control of multiple UAVs for forest fire detection and tracking mission, in: 2016 3rd Conference on Control and Fault-Tolerant Systems (SysTol), IEEE, 2016, pp. 133–138.
[19] Y. Zhang, Y. Zhang, Z. Yu, A solution for searching and monitoring forest fires based on multiple UAVs, in: 2019 International Conference on Unmanned Aircraft Systems (ICUAS), IEEE, 2019, pp. 661–666.
[20] The U.S. Air Force Research Laboratory, AMASE Tutorial session, 2010, https://github.com/afrl-rq/OpenAMASE.
[21] R. Luo, H. Zheng, J. Guo, Solving the multi-functional heterogeneous UAV cooperative mission planning problem using multi-swarm fruit fly optimization algorithm, Sensors 20 (18) (2020) 5026.
[22] A. Flenner, J. Flenner, J. Bobinchak, D. Mercier, A. Le, K. Estabridis, G. Hewer, Levy walks for autonomous search, in: Ground/Air Multisensor Interoperability, Integration, and Networking for Persistent ISR III, vol. 8389, International Society for Optics and Photonics, 2012, p. 83890Z.
[23] A. Dirafzoon, E. Lobaton, Topological mapping of unknown environments using an unlocalized robotic swarm, in: 2013 IEEE/RSJ International Conference on Intelligent Robots and Systems, IEEE, 2013, pp. 5545–5551.
[24] V. Fioriti, F. Fratichini, S. Chiesa, C. Moriconi, Levy foraging in a dynamic environment–extending the levy search, Int. J. Adv. Robot. Syst. 12 (7) (2015) 98.
[25] C. Garcia-Saura, E. Serrano, F.B. Rodriguez, P. Varona, Effects of locomotive drift in scale-invariant robotic search strategies, in: Conference on Biomimetic and Biohybrid Systems, Springer, 2017, pp. 161–169.
[26] D. Albani, D. Nardi, V. Trianni, Field coverage and weed mapping by UAV swarms, in: 2017 IEEE/RSJ International Conference on Intelligent Robots and Systems (IROS), IEEE, 2017, pp. 4319–4325.
[27] K. Harikumar, J. Senthilnath, S. Sundaram, Multi-uav oxyrrhis marina-inspired search and dynamic formation control for forest firefighting, IEEE Trans. Autom. Sci. Eng. 16 (2) (2018) 863–873.
[28] P. Vincent, I. Rubin, A framework and analysis for cooperative search using UAV swarms, in: Proceedings of the 2004 ACM Symposium on Applied Computing, ACM, 2004, pp. 79–86.
[29] H. Wollan, Incorporating Heuristically Generated Search Patterns in Search and Rescue, University of Edinburgh, 2004.
[30] P. LaValla, R. Stoffel, Search Is an Emergency: A Text for Managing Search Operations, Emergency Response Institute, 1990.
[31] O. Artemenko, O.J. Dominic, O. Andryeyev, A. Mitschele-Thiel, Energy-aware trajectory planning for the localization of mobile devices using an unmanned aerial vehicle, in: 2016 25th International Conference on Computer Communication and Networks (ICCCN), IEEE, 2016, pp. 1–9.
[32] M. Sulaiman, H. Liu, M. Binalhaj, W.W. Liou, O. Abudayyeh, GIS-Based automatic flight planning of camera-equipped UAVs for fire emergency response, in: 2020 IEEE International Conference on Electro Information Technology (EIT), IEEE, 2020, pp. 139–144.
[33] A. Chakrabarty, C.A. Ippolito, Wildfire monitoring using unmanned aerial vehicles operating under UTM (STEReO), in: AIAA Scitech 2021 Forum, 2021, p. 1472.
[34] E. Galceran, M. Carreras, A survey on coverage path planning for robotics, Robot. Auton. Syst. 61 (12) (2013) 1258–1276.
[35] G. York, D.J. Pack, Ground target detection using cooperative unmanned aerial systems, J. Intell. Robot. Syst. 65 (1–4) (2012) 473–478.
[36] H. Al-Helal, J. Sprinkle, UAV search: Maximizing target acquisition, in: 2010 17th IEEE International Conference and Workshops on Engineering of Computer Based Systems, IEEE, 2010, pp. 9–18.
[37] T.M. Cabreira, C. Di Franco, P.R. Ferreira, G.C. Buttazzo, Energy-aware spiral coverage path planning for uav photogrammetric applications, IEEE Robot. Autom. Lett. 3 (4) (2018) 3662–3668.

[38] F. Bourgault, T. Furukawa, H.F. Durrant-Whyte, Optimal search for a lost target in a bayesian world, in: Field and Service Robotics, Springer, 2003, pp. 209–222.
[39] S. Waharte, N. Trigoni, S. Julier, Coordinated search with a swarm of UAVs, in: 2009 6th Ieee Annual Communications Society Conference on Sensor, Mesh and Ad Hoc Communications and Networks Workshops, IEEE, 2009, pp. 1–3.
[40] S. Waharte, N. Trigoni, Supporting search and rescue operations with UAVs, in: 2010 International Conference on Emerging Security Technologies, IEEE, 2010, pp. 142–147.
[41] B. Grocholsky, J. Keller, V. Kumar, G. Pappas, Cooperative air and ground surveillance, IEEE Robot. Autom. Mag. 13 (3) (2006) 16–25.
[42] S. Waharte, A. Symington, N. Trigoni, Probabilistic search with agile UAVs, in: 2010 IEEE International Conference on Robotics and Automation, IEEE, 2010, pp. 2840–2845.
[43] T.a.M. Cabreira, P.R. Ferreira, C. Di Franco, G.C. Buttazzo, Grid-based coverage path planning with minimum energy over irregular-shaped areas with UAVs, in: 2019 International Conference on Unmanned Aircraft Systems (ICUAS), IEEE, 2019, pp. 758–767.
[44] D.W. Casbeer, D.B. Kingston, R.W. Beard, T.W. McLain, Cooperative forest fire surveillance using a team of small unmanned air vehicles, Internat. J. Systems Sci. 37 (6) (2006) 351–360.
[45] Y. Cheng, Mean shift, mode seeking, and clustering, IEEE Trans. Pattern Anal. Mach. Intell. 17 (8) (1995) 790–799.
[46] D. Comaniciu, P. Meer, Mean shift: A robust approach toward feature space analysis, IEEE Trans. Pattern Anal. Mach. Intell. 24 (5) (2002) 603–619.
[47] G. De Luca, J.a.M. N Silva, S. Cerasoli, J.a. Araújo, J. Campos, S. Di Fazio, G. Modica, Object-based land cover classification of cork oak woodlands using uav imagery and orfeo toolbox, Remote Sens. 11 (10) (2019) 1238.
[48] M. Duquette, The common mission automation services interface, in: Infotech@ Aerospace 2011, 2011, p. 1542.
[49] The swarm and search AI challenge: 2019 fire hack, 2019, https://fire-hack.devpost.com/.


**Mrinmoy Sarkar** received his B.S. degree in Electrical and Electronic Engineering from Bangladesh University of Engineering and Technology in 2016. He is currently pursuing his Ph.D. degree in Electrical and Computer Engineering at North Carolina A&T State University. He worked as a software engineer at Samsung R&D Institute Bangladesh Ltd. from July 2016–July 2017. His research interests include testing and evaluation of autonomous behavior of UAV agents using machine learning technique, developing different complex scenarios for testing UAVs and a heterogeneous system consisting of UAVs as well as UGVs, analyzing the behavior of large-scale autonomous systems and the application of machine learning techniques in robotics. He is a member of IEEE and Golden Key International Honour Society.

**Xuyang Yan** received his B.S. degree in Electrical Engineering from North Carolina Agricultural and Technical State University (NC A&T) and Henan Polytechnic University in 2016. In 2018, he earned his M.S. degree in electrical engineering at NC A&T. He is currently pursuing his Ph.D. degree in electrical engineering at NC A&T. His research interests include extracting knowledge from streaming data, analyzing the emergent behaviors of large-scale autonomous systems and the application of machine learning techniques in robotics.

**Berat Alper Erol** earned his B.S. degree in mathematics from Kocaeli University, his M.S. degree in software engineering from St. Mary's University, and his Ph.D. degree in electrical engineering from The University of Texas at San Antonio (UTSA), in 2007, 2012, and 2018, respectively. His doctoral research at UTSA Autonomous Control Engineering Laboratories has been sponsored by the U.S. Department of Defense (DoD), Air Force Research Laboratory (AFRL), Bank of America and 80|20 Foundation. After his doctoral program, he worked as a post-doctoral research associate in TECHLAV DoD Center of Excellence in Autonomy at North Carolina A&T State University, Greensboro, USA. During his post-doctoral assignment, Dr. Erol was a member of the team which delivered a DoD contract and worked in a few multi-institutional research grants including AFRL, Georgia Tech Research Institute, Lockheed Martin Corporation and NASA Langley Research Center. Currently, he is with the Computer Engineering department at the Izmir Institute of Technology, Izmir, Turkey. His current research interests include manned–unmanned teaming, intelligent robotics, testing and evaluation, human robot interactions, and Internet of Robotic Things. He is a Member of the IEEE, American Institute of Aeronautics and Astronautics, and IEEE Eta Kappa Nu honor society.

**Ioannis Raptis** joined the faculty of Electrical and Computer Engineering at North Carolina Agricultural and Technical State University as an Assistant Professor in Fall 2019. He is the director of the Autonomous Robotic Systems Laboratory (ARSL). Dr. Raptis received his Dipl-Ing. in Electrical and Computer Engineering from the Aristotle University of Thessaloniki, Greece, and his Master of Science in Electrical and Computer Engineering from The Ohio State University in 2003 and 2006, respectively. In 2010 he received his Ph.D. degree in the department of Electrical Engineering at the University of South Florida. Before joining NC A&T State University, Dr. Raptis held a Postdoctoral Fellow position at Georgia Institute of Technology, with a joint appointment in ECE and AE, and an Assistant Professor position in Mechanical Engineering at the University of Massachusetts Lowell.

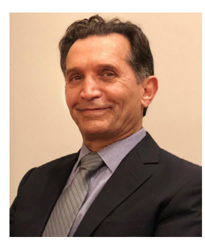

**Abdollah Homaifar** received his B.S. and M.S. degrees from the State University of New York at Stony Brook in 1979 and 1980, respectively, and his Ph.D. degree from the University of Alabama in 1987, all in Electrical Engineering. He is the NASA Langley Distinguished Professor and the Duke Energy Eminent professor in the Department of Electrical and Computer Engineering at North Carolina A&T State University (NCA&TSU). He is the director of the Autonomous Control and Information Technology Institute and the Testing, Evaluation, and Control of Heterogeneous Large-scale Systems of Autonomous Vehicles (TECHLAV) Center at NCA&TSU. His research interests include machine learning, unmanned aerial vehicles (UAVs), testing and evaluation of autonomous vehicles, optimization, and signal processing. He also serves as an associate editor of the Journal of Intelligent Automation and Soft Computing and is a reviewer for IEEE Transactions on Fuzzy Systems, Man Machines and Cybernetics, and Neural Networks. He is a member of the IEEE Control Society, Sigma Xi, Tau Beta Pi, and Eta Kapa Nu.